Space-resolved extreme ultraviolet emission from laser-produced plasmas

N. A. Ebrahim and M. C. Richardson
National Research Council of Canada, Division of Physics, Ottawa, K1A OR6, Canada

G. A. Doschek and U. Feldman
E. O. Hulburt Center for Space Research, Naval Research Laboratory, Washington, D.C. 20375

(Received 29 June 1979; accepted for publication 24 August 1979)

We have obtained extreme ultraviolet (XUV) spectra of plasmas created by focusing nanosecond CO_2 laser pulses onto massive planar targets of Al, Ti, and CH_2. The instrument used to obtain these spectra was a normal incidence extreme ultraviolet spectrograph with the entrance slit removed. The cancave spherical grating of such a slitless spectrograph diffracts and focuses the XUV radiation, and the resulting images are recorded on Kodak 101 film. The XUV images are therefore space resolved but time averaged over the lifetime of the plasma. The wavelength range covered in these spectra is 200– 500 Å. In this range, the emission lines of aluminum are due to transitions between the $2s^2 2p^k$, $2s2p^{k+1}$, and $2p^{k+2}$ configurations within the ions from Al V through Al X. For titanium plasmas, emission lines from Ti VII, Ti XI, and Ti XII have been identified. The prominent images obtained from polyethylene plasma result from $2l$-$3l'$ and $2l$-$4l'$ transitions within the CIV ion. The general morphology of the plasma expansion shows that the most highly ionized species (Al X, Ti XII) expand away from the target surface in well-collimated cylindrical structures. These most highly ionized species also exhibit two component structures; one component expanding along the target normal and the second component expanding parallel to the incident laser direction. The images of the low-ionization stages (Al V, Ti VII) are also cylindrical although their spatial extent is much less than the images from the high-temperature ions and they are not as well collimated. The observations are interpreted in terms of particular temperature structues in such plasmas and the presence of self-generated magnetic fields.

PACS numbers: 52.25.Ps

INTRODUCTION

The interaction of intense electromagnetic radiation with solid targets *in vacuo* generates high-density high-temperature plasmas. Such high-energy plasmas are of considerable topical interest not only because of their importance in thermonuclear fusion research but also because they provide a source of highly stripped ions for a wide range of studies in laboratory astrophysics, atomic physics, and extreme ultraviolet (XUV) emission spectroscopy. These plasmas have also been considered as possible lasing media for soft x-ray lasers. A basic experimental approach common to all studies of plasmas of this type is to undertake a global series of experimental measurements and interpret them in terms of currently available theories and results of hydrodynamic and PIC simulation studies. The range of diagnostics commonly deployed in such experimental studies include picosecond interferometry, measurements of absorbed and reflected laser radiation, x-ray emission (line and continuum), spectra of plasma emission at the frequency of the incident laser radiation and its harmonics, and the spectra of fast electrons and ions. A very large body of experimental data now available from various laboratories makes it possible to describe the basic characteristics of laser-produced plasmas, despite the fact that a full understanding of the processes which govern the general behavior of such plasmas is far from complete.

In this paper we report the results of a study of laser-produced plasmas in the XUV spectral range (200–500 Å) using a recently developed diagnostic technique.[1–4] The relevance of this study and, in particular, the diagnostic technique at the present time to laser fusion investigations rests in its possible application to the investigations of ablative behavior in thin foil targets and microspheres, where the implosion velocities and plasma temperatures obtained are generally lower than those encountered in the more usual exploding pusher behavior. The lower temperatures created in such plasmas result in lower x-ray fluences, thus limiting the use of conventional x-ray diagnostic techniques. However, useful studies of the emission characteristics of such plasmas can still be made at longer wavelengths by observing the emission from the lower temperature ions which emit quite strongly in the XUV region. In the past, XUV spectra in this region have been obtained using a normal incidence spectrograph, and by positioning the target at the Sirk focus, spatial resolution in one dimension has been achieved.[5] The present technique eliminates the slit altogether. The concave spherical grating produces two-dimensional images of the plasma in discrete XUV lines, so that a complete map of the XUV emitting regions of the plasma can be obtained in a single laser shot. This method of photographing the plasma in two dimensions at discrete wavelengths reveals some unusual and interesting features in the XUV emission from laser-produced plasmas which have not been observed previously with slit spectrographs. The only constraint on the use of slitless spectrographs is that the spectral lines be selected such that the neighboring images do not overlap significantly. Since the XUV spectrum of ions of elements up to $Z = 28$ is well known from analyses of solar and laboratory plasmas,

 0021-8979/80/010182-08$01.10

and there are many strong spectral lines that can be emitted between 200 and 600 Å for most values of Z, it is possible to carefully select the lines being observed before hand, so that this constraint does not pose a serious problem at all.

In a previous study[1] monochromatic images of laser-produced plasmas were obtained in the XUV region between 200 and 550 Å. The plasmas were produced by focusing a 1.06-μm high-power Nd : glass laser onto flat targets of various elements. XUV emission in such plasmas was observed as far away as 1 cm from the target surface, and several rather unusual features were observed in the emission structures. For instance, the emission from Ti XII lines shows that the plasma does not expand in a hemispherical or conical plume. Instead, the expansion is well collimated and highly directional. Some of the images show definite structures. One component in the emission feature expands backward along the incident laser pulse direction, and a second component expands at an angle between this direction and the target normal. Finally, these studies revealed the differing behavior of plasmas produced by irradiating metallic and dielectric targets. Whereas the emission from plasmas formed from Ti and Al targets appear as narrow cylindrical structures, the expansion features from polyethylene targets are broad fanlike structures.

Similar investigations[2] of plasmas produced by a gain-switched CO_2 laser showed very different behavior in the plasma expansion to that observed in Nd : glass laser-produced plasmas. In particular, the emission from the most highly ionized species was observed to be along the direction of the target normal, whereas the expansion of the lower Z species was always along a direction parallel to the incident laser pulse direction. This spatial separation of high and low Z ions is perhaps not altogether surprising considering that the CO_2 laser pulse was relatively long (70 ns FWHM), followed by a long 1-μs low-intensity tail. Such behavior would seem to be consistent with a picture in which the highly ionized species were produced in the hot plasma during the 70-ns initial spike, and the low Z ions resulted from the cooler plasma formed during the long tail of the laser pulse.

The chief motivation behind the present studies was to obtain XUV spectra from plasmas produced by a nanosecond CO_2 laser pulse and to compare these with spectra obtained from plasmas produced by other laser systems in terms of the wavelength of the laser radiation, laser pulse lengths, and maximum intensities. A large number of target materials were used to see the dependence of such spectra on the metallic or dielectric properties of the target material and to observe any variations of the general plasma morphology with heavy and light elements. Finally, we consider some simple models of the plasma behavior which would result in the observed emission spectra and which would be consistent with the experimentally observed characteristics of such plasmas.

II. EXPERIMENT

The experiments were performed with a single beam of the COCO-II laser system which includes an actively mode-locked oscillator and a number of uv preionized atmospheric pressure CO_2 amplifier modules.[6] The approximately Gaussian shaped pulse from the oscillator is considerably modified by saturation effects in the amplifier chain and by the in-line saturable absorber cells. Prepulse levels greater than 50 μJ and prelase levels greater than 50 kW can be detected in this system, and the pulse contrast ratio is approximately 10^6.

Flat massive targets were illuminated by the output of the laser system [35 J, 1.5 ns (FWHM)] focused to a half-energy diameter of 110 μm with $f/2.5$ off-axis parabolic optics. This provided peak intensities of 2×10^{14} W/cm^2 on target, with prepulse radiation levels of no greater than 2×10^8 W/cm^2. Under these conditions, picosecond visible light interferometry[7] confirmed that prior to irradiation by the main laser pulse there existed no plasma at the target surface with electron density in excess of 10^{18} cm^{-3}.

Investigations of the plasmas with a picosecond interferometric probe at conditions quite similar to those used in the present experiments give the characteristics of the electron density distribution throughout the laser pulse and during the plasma decay phase following the pulse. These studies show clear evidence of profile modification due to pondermotive forces, with a steep density gradient having a scale length during the laser pulse of approximately 10 μm from $0.2n_c$ to $7n_c$ at 2×10^{14} W/cm^2. The development of deep density craters[8] has also been observed during the interaction, where the plasma directly in the path of the photon beam is pushed back towards the high-density region as a result of transverse intensity variations, across the laser beam. It is possible that these density wells and the general rippling of the critical density surface are at least, in part, responsible for some of the structure that is observed in the XUV emission spectra discussed later.

Line intensity ratio measurements[9] in the x-ray region have indicated a thermal temperature of 350–400 eV in the high-density plasma ($n_e > 10^{19}$ cm^{-3}). Assuming that the highest ionization stages are formed in the focal region, a

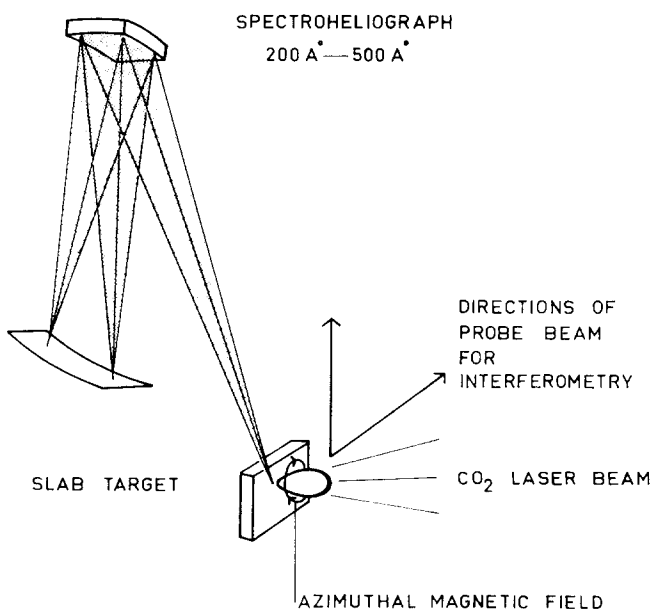

FIG. 1. Schematic of the experimental arrangement.

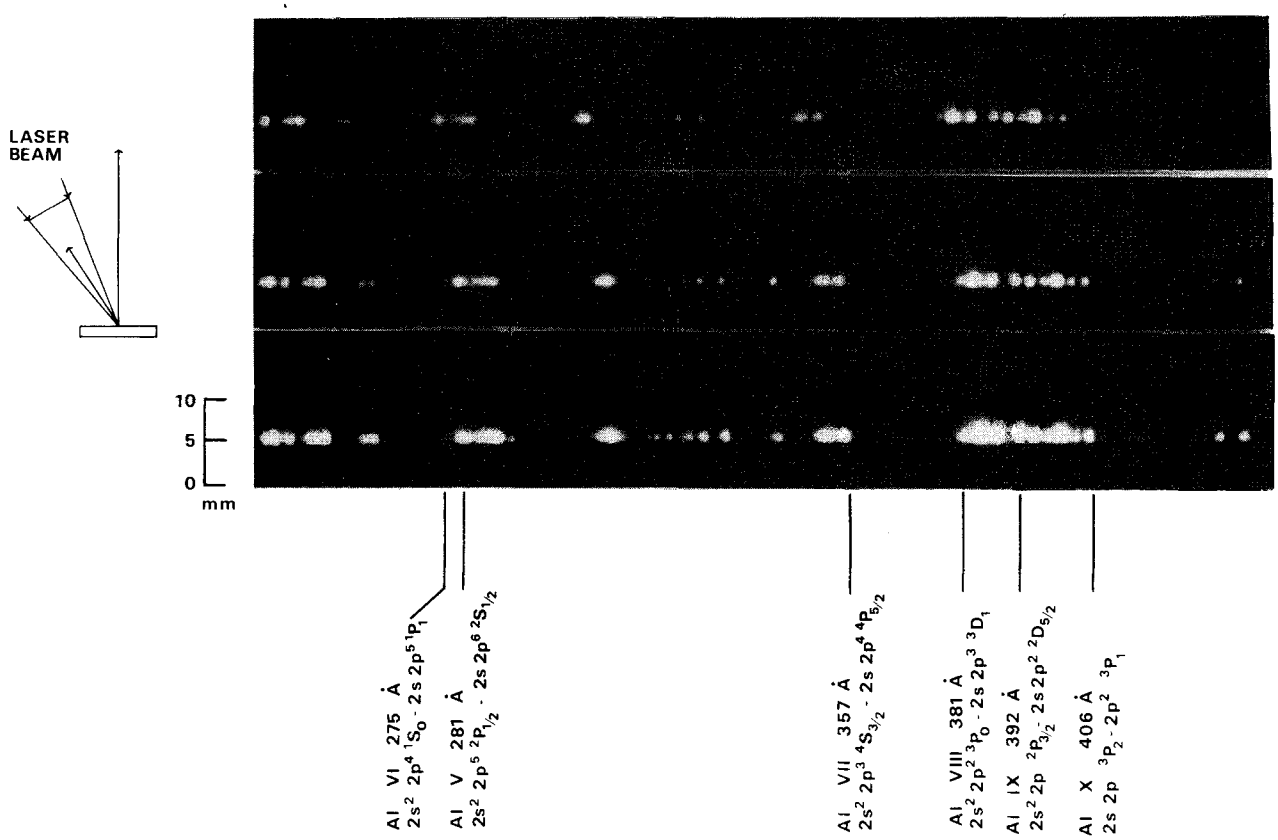

FIG. 2. Three spectra of CO_2 laser-produced plasmas obtained with aluminum targets. The target normal was tilted 35° to the incoming direction. The millimeter scale gives distances from the target surface.

temperature of approximately 400 eV is consistent with the observation of H and He-like aluminum. As will be shown, the temperature at distances of several millimeters from the target surface can be estimated from the presence of low-temperature ions. From these observations the electron temperatures are of the order of 100 eV.

The spectra in this study were obtained using a slitless extreme ultraviolet spectrograph (spectroheliograph) described earlier,[1-4] operating in the 200–500-Å spectral range. The spectroheliograph produces two-dimensional images of the plasma in discrete XUV emission lines which are recorded on Kodak 101 film and are therefore time averaged over the plasma lifetime. For these experiments the spectroheliograph was deployed as in Fig. 1, where the source-grating distance was 165 cm and grating-film distance was 72 cm, giving a magnification of 0.43 and a reciprocal dispersion at the film of 3.89 Å/mm. The astigmatic blur in the focal plane along the direction of plasma expansion at a wavelength of 300 Å is less than 22 μm, and this limits the spatial resolution in this direction to about 50 μm. In the direction of dispersion the blur is 10 μm and the corresponding spatial resolution is bout 23 μm.

III. RESULTS

A. Description of spectroheliograms

Figure 2 shows three typical spectra from an aluminum target. Each spectrum was obtained with a single 1.5-ns CO_2 laser pulse of $\sim$35 J energy. In the wavelength range of these spectra (250–440 Å) the aluminum emission lines result from transitions between the $2s^2 2p^k$, $2s2p^{k+1}$, and $2p^{k+2}$ configurations within the ions of Al V through Al X. A comparison of the aluminum spectrum with the theoretical spectrum[10] shows that quite a few of the images are, in fact, blends of several emission lines, some of which origniate from different ionization stages. Only when the plasma dimensions are small enough such that the extent of the XUV image along the direction of dispersion is small, can many of the lines be clearly resolved. For example, such is the case for plasma produced from thin foil targets of dimensions comparable to the focal spot diameter.

The continuous emission close to the target surface is free-free and free-bound continuum. The plasma expands as shown in Fig. 2 in narrow cylindrical plumes, and emission can be observed up to about 6 mm from the target surface. Normal to the target surface the resolution is purely spatial, while parallel to the target surface the resolution is both spatial and spectral. The maximum contribution of thermal ion Doppler broadening to the image size, for Te$\simeq$400 eV and $\lambda = 461$ Å, is approximately 60 μm at the target surface. Doppler broadening due to the expansion velocity, likewise, contributes less than 50 μm to the image size for a velocity of about 2×10^7 cm/s.[4] Thus, the resulting spectral image quite accurately portrays the shape of the plasma in both directions. For these experiments the target normal was tilted 35° to the incoming beam direction, as shown in Fig. 2.

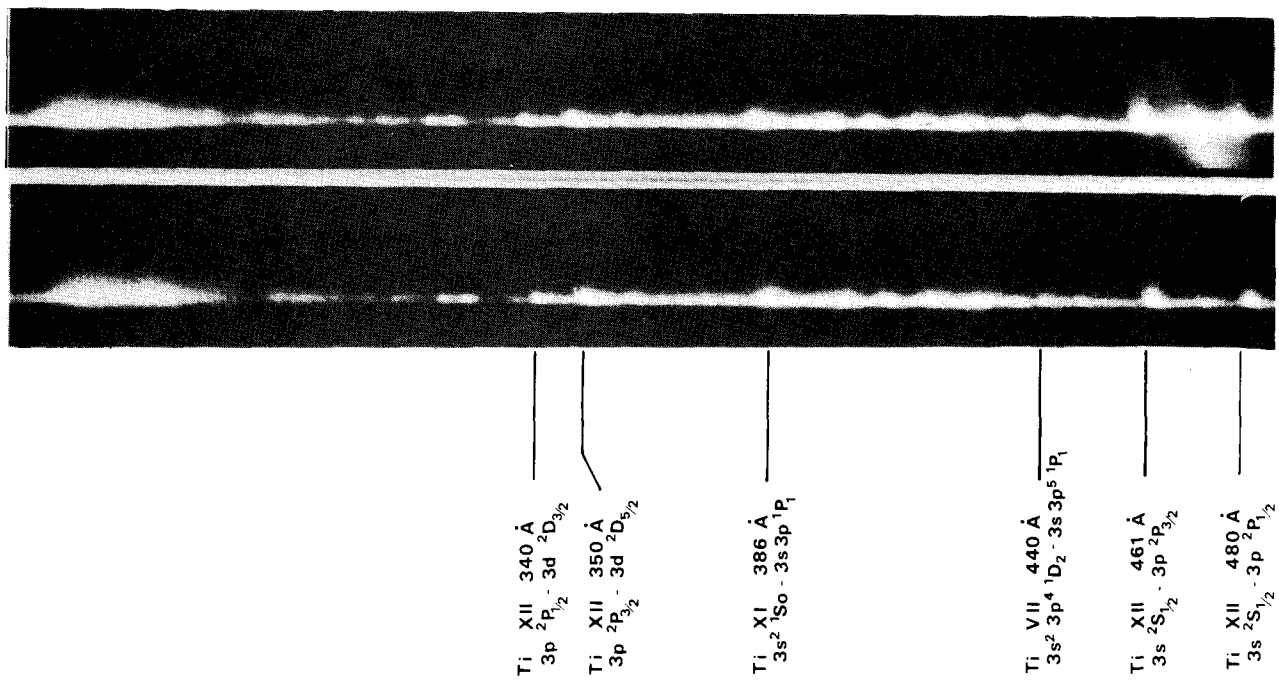

FIG. 3. Two spectra of CO_2 laser-produced plasmas obtained with titanium targets. The density sensitive lines in the Na isoelectric sequence are shown in these spectra.

It is seen from Fig. 2 that the plumes are either narrow cones or narrow cylinders. Generally, the most highly ionized species, e.g., Al IX and Al X, appear as narrow cylinders, whereas the less ionized species, e.g., Al V, Al VI, and Al VII, have a conelike or cylindrical structure of greater radius. This is clear from Fig. 2 if one compares the Al X images (at 406.4 Å) to Al VII images (at 356.9 Å).

Figure 3 shows two spectroheliograms obtained from Ti targets. The energy in the laser pulse on target was 39 J for the upper spectrum and 42 J for the lower one. For the top spectrum the target was a 3-mm-diam cylinder of titanium while the lower spectrum was obtained from a cylindrical titanium target about 200 μm in diameter. Images of Ti VII, Ti XI, and Ti XII have been identified in these spectra. Figures 4 and 5 show two-dimensional photographic isodensity contour plots of the images of two of the transitions in the lower spectrum shown in Fig. 3.

In these spectra the line emission from the 3*s*-3*p* lines of Ti XII at 480 and 461 Å is confined to a narrow cylinder (having a diameter of between 500 and 800 μm) directed back in the general direction of the incident laser pulse. In some cases emission can be observed as far away as 8 mm from the target surface. Another interesting feature of these spectra is that the images of the most highly ionized species show a two-component structure. One component lies along the target normal and the second component in a direction between the target normal and the incident laser pulse. The less ionized species, on the other hand, do not extend too far from the target surface and generally appear as brighter regions in the continuum. As in the case of aluminum, emission from the lower ionization stages in both cases does not appear to be as sharply collimated as is the case with the higher ionization stages. The low ionization stages are prob-

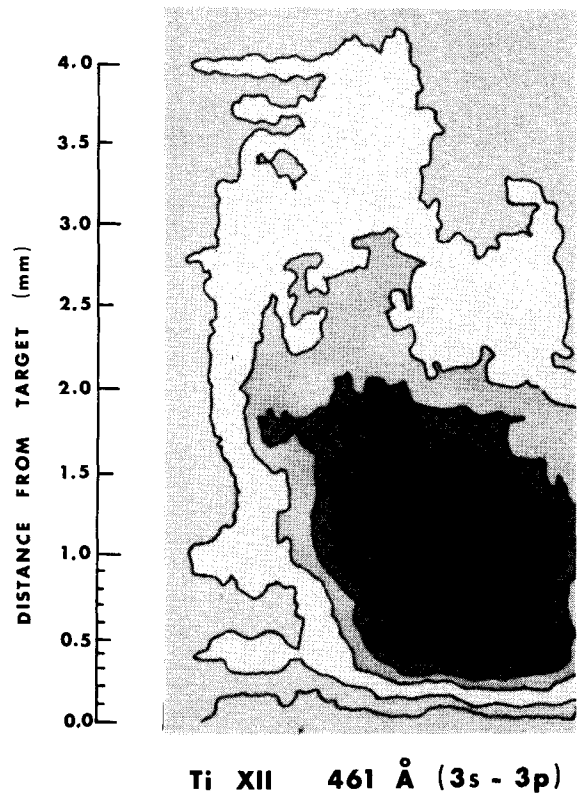

FIG. 4. The isodensity contour plot of the Ti XII image at 461 Å shown in the spectrum of Fig. 3. The shadings indicate areas of equal photographic density, black corresponding to the highest density.

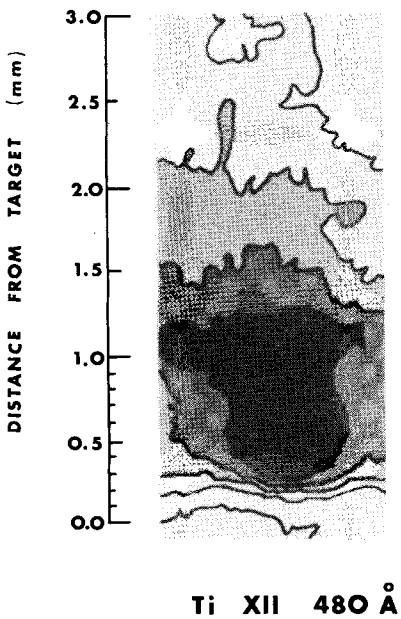

FIG. 5. The isodensity contour plot of the Ti XII image at 480 Å shown in the bottom spectrum of Fig. 3.

ably formed as a result of recombination from higher ionization stages and exist in the cooler plasma at much later times after the laser pulse.

Figure 6 shows a spectroheliogram obtained from a polyethylene target. The energy on target in this case was about 42 J and the target was a polyethylene disk approximately 3 mm in diameter. The prominent emission features obtained in this spectral region from a polyethylene plasma are the C IV images. These images are due to $2l$-$3l'$ and $2l$-$4l'$ transitions in the C IV ion. From Fig. 6 we note that in the case of a polyethylene plasma the expansion appears to be fanlike, in the form of a wide-angle cone centered about the incident laser direction. There is no evidence of any structure in these particular images. This rather broad expansion obtained with carbon images has also been observed elsewhere.[1,11] XUV images of the more-highly-ionized carbon ions have been obtained recently[12] using a dispersive microscope operating in the region of ~ 100 Å. The images of the H_α line of C VI at 182 Å obtained using such a device appear more like a conical plume than a broad fanlike structure, as is the case with C IV images. It is therefore clear that with metallic and dielectric targets the ions of higher ionization exist in the much narrower regions of the plume.

The one-dimensional expansion observed in the XUV emission from Nd : glass and CO_2 laser-produced plasmas tends to suggest the presence of a radially confining force in these plasmas. Such a force can result from large-scale azimuthal self-generated magnetic fields, and we have shown recently that the various features observed in the XUV spectra of nanosecond CO_2 laser-produced plasmas are, in fact, quite consistent with the presence of such fields.[4] The essential point in these analyses is that MHD effects will directly influence the plasma dynamics in the regions of $\beta < 1$, where β is defined as the ratio of the plasma pressure to the magnetic pressure ($= 2\mu_0 N_e kT/B^2$). The time-averaged electron temperature in the Nd : glass laser-produced plasmas, as determined from x-ray spectra for conditions similar to those obtained in the XUV studies was 650 eV[1]. Assuming that the maximum value of the fields occur at approximately $n_e = 0.1 n_c$ (where $n_c = 10^{21}$ cm^{-3}), $\beta = 1$ for $B = 1.6$ MG. Experimentally, such fields have been observed recently by Faraday rotation in Nd : glass laser-prodcued plasmas[13,14] for values of $I\lambda^2$ quite similar to those in the studies discussed in this paper. For instance, maximum field amplitudes of 1.8 MG off aluminum targets irradiated by a Nd : glass laser at an intensity of 1×10^{16} W/cm^2 with an electron density in the region of the maximum field of $0.16 n_c$ have been measured.[14] It is therefore clear that such magnetic fields can be expected to modify the density profile in these plasmas quite appreciably.

We should also point out that spectroheliograms obtained from 150- and 500-μm spherical targets irradiated on one side with a nanosecond CO_2 laser pulse also show the one-dimensional expansion in the XUV emission.[15] However, Faraday rotation measurements on small microballoon targets under 1.06-μm irradiation do not show evidence of magnetic fields within the system sensitivity of 100 kG.[14] This is attributed to that fact that on small targets with diameters of the order of the focal-spot size, the symmetry of the spherical expansion results in small source terms for magnetic fields. On large spherical targets the nonspherical symmetry due to the nonuniform irradiation can result in large enough source terms and hence significant magnetic fields.

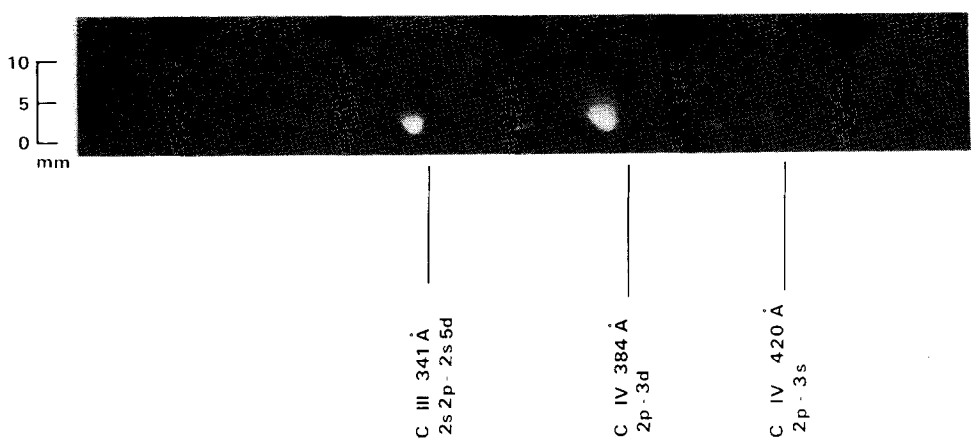

FIG. 6. Spectra of CO_2 laser-produced plasmas obtained with CH_2 targets.

Experiments with Nd : glass lasers using large (100 μm) spherical targets and small (25 μm) focal spot have, in fact, detected magnetic fields of up to 1.5 MG.[13]

A second possibility lies in the assumption that the general shape of the expanding plume is a cone, with the most highly ionized species occupying the center of the cone. Lower temperature regions will form successive overlapping shells around this high-temperature region. This is certainly possible because of the radial energy distribution of the laser focal spot. This type of a temperature structure has, in fact, been found[11] for polyethylene targets irraditated by a 5-J 17-ns ruby laser with an average intensity of 2.9×10^{11} W/cm^2. However, this explanation is not completely satisfactory in the case of heavier elements where even the images of the lower ionization stages tend to be cylindrical in appearance and where the temperature structure that must exist in order to produce this behavior can no longer be explained simply on the basis of the radial energy distribution within the laser focal spot.

B. Comparison with spectroheliograms obtained with other laser systems

As pointed out earlier, spectroheliograms of plasmas produced off Al, Ti, and Fe targets have also been obtained at NRL with two laser systems having distinctly different characteristics from that used in the present study. The NRL Nd : glass laser delivered a 10-J 100–500-ps, 1.06-μm pulse, focused by an $f/1.9$ lens to focal spot dimensions of $\sim$20 μm, providing peak intensities of greater magnitude ($\sim10^{16}$ W/cm^{-2}) but of comparable value in ($I\lambda^2$), for a similar time period, as the NRC laser system. The second NRL system was a gain-switched CO_2 laser system producing a 300-MW 70-ns duration pulse followed by a low-intensity long (1 μs) 40-MW tail, focused to comparable focal dimensions ($\sim$200 μm) but providing peak intensities ($\sim10^{12}$ W/cm^{-2}) considerably less than the present CO_2 laser system, but over a time period in which significant interaction of the laser beam would occur during the expansion phase of the plasma. All three studies were performed with the same spectroheliograph, and it is therefore instructive to compare the spectroheliographs obtained in all these studies.

The NRL spectroheliograms of Al have recently been described.[10] They found little if any difference in relative line intensitites between the short-pulse Nd : glass and the long-pulse CO_2 laser spectra. We, in turn, find no difference in relative line intensities between the short-pulse CO_2 laser spectra and the NRL results. The reason for this revolves around the temperature and density of the laser plasmas and the spectroscopy of Al. Within the range of the spectroheliograph ($\simeq$200–500 Å) fall the lines of Al V through Al X. The lines of Li-like Al XI fall between 550 and 568 Å, while strong lines of Al XII and Al XIII fall in the x-ray region. The ions Al^{+4} through Al^{+9} are easy to produce at the

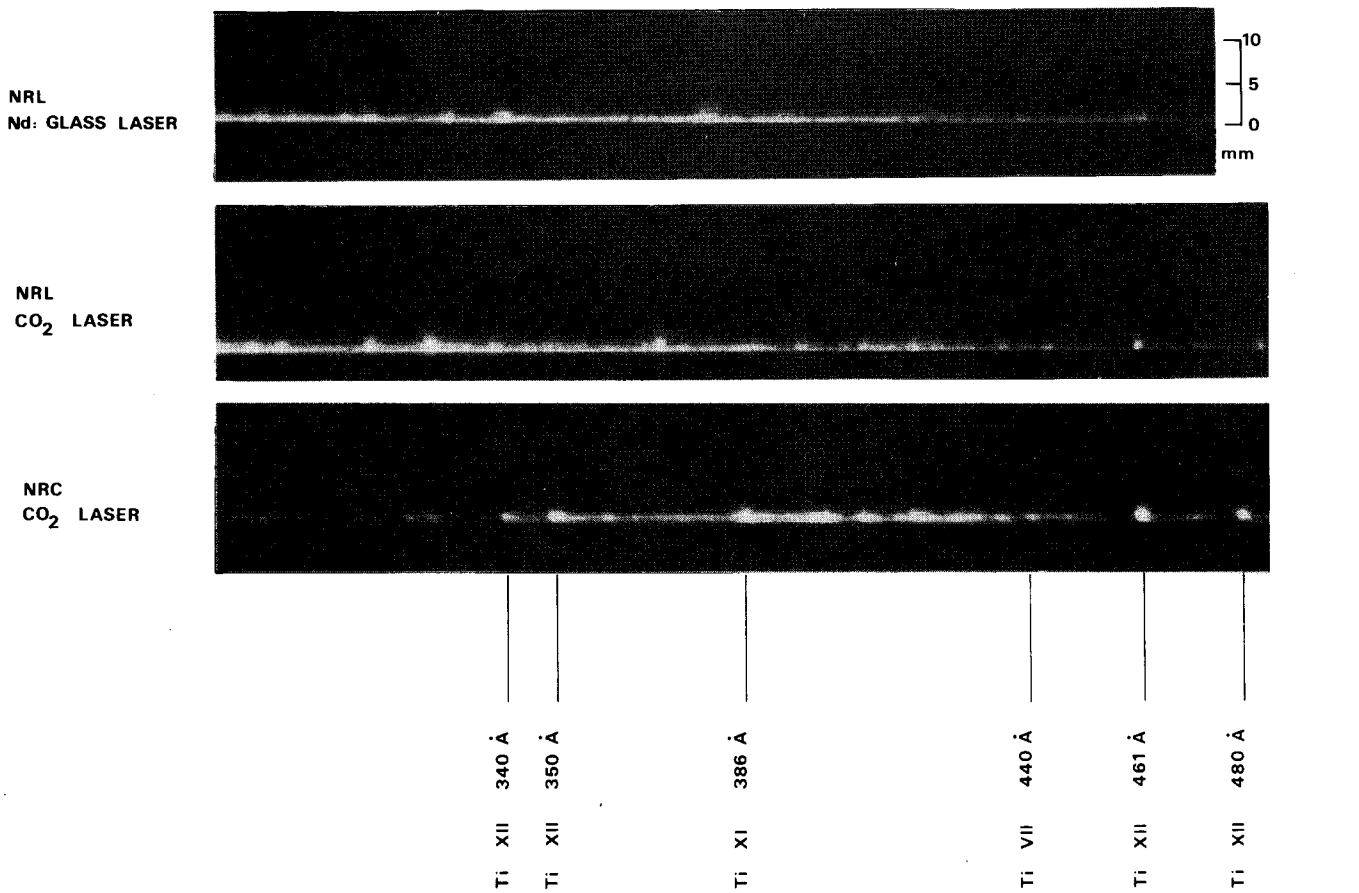

FIG. 7. Comparison of laser-produced plasma spectra of titanium targets obtained with NRL Nd : glass laser (upper spectra), NRL gain-switched CO_2 laser (middle spectra), and NRC short-pulse CO_2 laser (lower spectra).

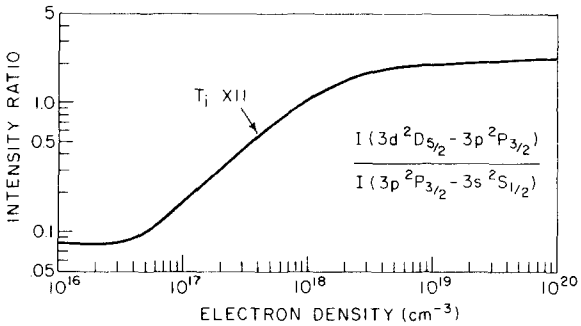

FIG. 8. Intensity ratio (erg) of the spectral lines in the Na-I isoelectronic sequence for Ti as a function of electron density.

temperature of the glass and CO_2 laser plasmas. Spectra of Al^{+11} are observed in the x-ray region. Furthermore, Al is a rather light element, and typical transition probabilities for transitions between the $2s^2 2p^k$, $2s2p^{k+1}$, and $2p^{k+2}$ configurations are of the order of $\gtrsim 5\times 10^9\ s^{-1}$. (Transitions betwen these configurations are responsible for the emission lines observed in the spectroheliograms.) Now the densities of CO_2 plasmas are $\gtrsim 10^{17}\ cm^{-3}$, while densities in Nd : glass laser plasmas are $\gtrsim 10^{19}\ cm^{-3}$. At densities above $\approx 1\times 10^{18}\ cm^{-3}$ the product of the density N_e times the electron impact excitation coefficients C_{ij} for excitations between levels of the above-mentioned configurations is comparable to or greater than the transition probabilities. Thus, the levels of these three configurations at densities $> 10^{18}\ cm^{-3}$ are in relative Boltzmann equilibrium for each ion, and therefore all the Al spectra look very similar. However, far from the target where $N_e \approx 10^{17}\ cm^{-3}$ this condition is not true. The low-density region appears to be about 1 mm away from the target surface in our spectra. Spectra of elements such as Al are useful for studying the morphology of the plasma expansion and for determining the wavelength efficiency of the spectroheliograph.[10]

As shown in Fig. 7, a comparison of the Ti spectra produced by the three laser systems reveals significant differences. In the nanosecond CO_2 laser spectra, the Ti XII at 461 Å is about as intense as the Ti XII image at 350 Å in the target region. The line intensity ratios of the Ti XII 350- or 341-Å lines to the Ti XII 461-Å is density sensitive. The theoretical sensitivity is given in Fig. 8,[1] and this implies a density of about $10^{18}\ cm^{-3}$. In the NRL CO_2 spectra, the 461-Å image away from the target is brighter than the shorter-wavelength images, but close to the target surface the intensities are about equal. This implies a similar density near the target surface in the NRL CO_2 plasmas. In the NRL glass spectra, the 341- and 350-Å images are stronger than the 461-Å image, implying densities of at least $5\times 10^{18}\ cm^{-3}$. This is expected since most of the plasma heating occurs at a density of 10^{21} and $10^{19}\ cm^{-3}$ for glass and CO_2 laser, respectively. Most of the line emission in the CO_2 laser plasmas appears to occur at densities about an order of magnitude less than the critical density.

The time-integrated distribution of Ti ions in the spectra of all these laser systems is qualitatively quite similar. The intensity of the Ti XI image at 386 Å is about the same as the Ti XII images just discussed. In the nanosecond CO_2 laser spectra, well-resolved images of Ti XI and lower degrees of ionization appear between 386 and 460 Å. These are not nearly as apparent in the NRL glass laser spectra, and this may result from a higher temperature of the Nd : glass laser plasma. The Li-like Ti XX images are not present in the CO_2 spectra. Assuming ionization equilibrium, this implies a maximum electron temperature of about 1 keV for the CO_2 laser plasmas.

The axial extent of the short-pulse CO_2 laser Ti and Al images beyond the target and the extent of the NRL Nd : glass Ti and Al images are about the same. On the other hand, the NRL CO_2 images, which are also cylindrical in shape, are substantially longer or more extended away from the target than in the NRC spectra.[2] We believe that this could be a result of the much longer pulse length of the NRL CO_2 laser than the pulse lengths of the NRC laser or the NRL Nd : glass laser. For the CO_2 laser, the Ti images extend about 3.5 mm from the target. In the case of the NRL Nd : glass laser, the images extend about 2.5 mm.

IV. CONCLUSIONS

We have obtained XUV spectra of laser-produced plasmas created by focusing nanosecond CO_2 laser pulses onto massive planar targets of Al, Ti, and CH_2. The instrument used to obtain these spectra was a slitless normal incidence extreme ultraviolet spectrograph covering the wavelength range 200–500 Å.

The general morpholgy of the plasma expansion shows that the ions of higher multiplicity expand away from the target surface in well-collimated cylindrical structures, which observation is consistent with the presence of self-generated magnetic fields in such plasmas. We have also shown that the highly ionized species exhibit two-component structures, one component expanding along the target-normal and the second component expanding parallel to the incident laser direction. It is possible that density craters and the genreal rippling of the critical density surface are at least, in part, responsible for the structures that are observed in these spectra. A comparison of Al spectra obtained with Nd : glass and CO_2 lasers show very little difference in the relative line intensities. This behavior is explained in terms of the temperature and density of the laser plasmas and the spectroscopy of Al. A similar comparison of Ti spectra shows that while the time-integrated distribution of Ti ions is qualitatively quite similar, there are significant differences in the relative line intensities, reflecting the different densities at which plasma heating occurs in Nd : glass and CO_2 laser plasmas. Finally, it is suggested that the present diagnostic technique may be useful in the investigations of ablative behavior in thin foil targets and microspheres where the lower temperatures result in lower x-ray fluences, thus limiting the use of conventional x-ray diagnostic techniques.

ACKNOWLEDGMENTS

The authors wish to thank Dr. C. Joshi and Dr. G.D. Enright for many useful discussions, and P. Burtyn, G.A. Berry, and Y.P. Lupien for their continuing technical support.

[1]U. Feldman, G.A. Doschek, D.K. Prinz, and D. Nagel, J. Appl. Phys. **47,** 1341–50 (1976).
[2]G.A. Doschek, U. Feldman, P.G. Burkhalter, T. Finn, and W.A. Feibelman, J. Phys. B **10,** 745 (1977).
[3]N.A. Ebrahim, U. Feldman, G.A. Doschek, M.C. Richardson, and G.D. Enright, Bull. Am. Phys. Soc. **23,** 838 (1978).
[4]N.A. Ebrahim, M.C. Richardson, R. Fedosejevs, and U. Feldman, Appl. Phys. Lett. **35,** 106 (1979).
[5]B.C. Boland, F.E. Irons, and R.W.P. McWhirter, J. Phys. B Ser. 2, **Vol. 1,** 1180–91 (1968).
[6]M.C. Richardson, N.H. Burnett, H.A. Baldis, G.D. Enright, R. Fedosejevs, N.R. Isenor, and I.V. Tomov, *Laser Interaction and Related Plasma Phenomena*, edited by H.J. Schwarz and H. Hora (Plenum, New York, 1977), Vol. 4a, p. 161.
[7]R. Fedosejevs, I.V. Tomov, N.H. Burnett, G.D. Enright, and M.C. Richardson, Phys. Rev. Lett. **39,** 932 (1977).
[8]R. Fedosejevs, M.D.J. Burgess, G.D. Enright, and M.C. Richardson, Bull. Am. Phys. Soc. **23,** 768 (1978).
[9]G.D. Enright, N.H. Burnett, and M.C. Richardson, Appl. Phys. Lett. **31,** 494 (1977).
[10]G.A. Doschek and U. Feldman (unpublished).
[11]F.E. Irons, R.W.P. McWhirter, and N.J. Peacock, J. Phys. B **5,** 1975 (1972).
[12]G.V. Pergudov and E.N. Ragozin, JETP Lett. **28,** 26 (1978).
[13]J.A. Stamper, E.A. McLean, and B.H. Ripin, Phys. Rev. Lett. **40,** 1177 (1978).
[14]A. Raven, O. Willi, and P.T. Rumsby, Phys. Rev. Lett. **41,** 554 (1978).
[15]C. Joshi and N.A. Ebrahim (unpublished).